Supplementary Information for

Electrochemical Host-Guest Interactions in a Disordered Oligosilyl Coordination Polymer

Rasha I. Anayah[1], Brian G. Diamond[3], Christopher H. Hendon*[3], V. Sara Thoi*[1,2]

[1]Department of Chemistry, Johns Hopkins University, Baltimore, MD

[2]Department of Materials Science and Engineering, Johns Hopkins University, Baltimore, MD

[3]Department of Chemistry and Biochemistry, University of Oregon, Eugene, OR

*Corresponding Author: sarathoi@jhu.edu, chendon@uoregon.edu

Table of Contents

Experimental Details

General Materials. $ZrCl_4$ (Strem, 99%), n-butyllithium (Aldrich, 2.5M in hexanes). 1,4-dibromobenzene (Combi-blocks, 98%). Diethyl ether (Fisher, 99%). Magnesium sulfate (Fisher Scientific, 98%). N,N-dimethylformamide (Sigma Aldrich, 99.8%). Formic Acid (Acros Organics, 97%). 7,7,8,8-tetracyanoquinodimethane (Aldrich, 98%). Tetrabutylammonium hexafluorophosphate (Sigma Aldrich, > 99%).

General instrumentation. Powder X-ray diffraction was conducted on between Bruker D8 Focus diffractometer, Cu Kα, LynxEye detector from 2θ = 5-60ºC. Thermogravimetric analysis (TGA) was conducted using a TA Instruments SDT Q600 under flowing air from 20 ºC to 800 ºC at a heating rate of 5.0 ºC per minute. Diffuse Reflectance UV-vis spectroscopy was done with a Cary 5000 UV-vis NIR Spectrophotometer with attached integrating sphere. Attenuated total reflectance infrared spectroscopy (ATR-IR) was done on ThermoScientific Nicolet iS FT-IR with iD 5 ATR attachment. Cyclic voltammetry (CV) was done on an Ivium-n-STAT multichannel electrochemical analyzer. The potential was cycled between -1.5 V and 1.8 V vs Ag. Scanning Electron Microscopy (SEM) SEM images were collected using a JEOL JSM IT100 Scanning Electron Microscope, and samples were mounted on copper tape. Solid-state Magic Angle Spinning (MAS) NMR was collected using a 500 MHz Bruker Spectrometer and collected at 20 kHz in a Phoenix probe.

Synthesis of lin-Si-2. Following a previously reported synthesis of the lin-Si-2 ligand[1], 2.0 eq of 1,4-dibromobenzene (8.033 mmol, 1.895 g) was dissolved in 20mL of diethyl ether in a 100 mL Schlenk flask. The flask was cooled to 0ºC in an ice water bath and 2.0 eq of 2.30 M *n*-BuLi (8.03 mmol, 3.8 mL) was added dropwise via syringe to the solution while stirring. After 2 h, 1.0 eq of 1,2-dichlorotetramethyldisilane (4.01 mmol, 0.75 mL) was added dropwise via syringe to the solution and stirred and warmed to room temperature overnight. The reaction was then quenched with 10 mL of saturated ammonium chloride. The aqueous layer was extracted with diethyl ether (3x 20 mL) and the organic layer dried over magnesium sulfate and the solvent was evaporated under a reduced pressure. The resulting oil was then recrystallized in the freezer and the solids were collected via vacuum filtration (labeled S-2). The crystals were then dissolved in 20mL of diethyl ether in a 100 mL Schlenk flask. The flask was cooled to 0ºC in an ice water bath and 2.0 eq of 2.30 M n-BuLi (4.04 mmol, 1.6 mL) was added dropwise via syringe to the solution while stirring. After 2 h, 40 mL of toluene was added to the solution and dry ice was sublimed through a Drierite column and bubbled into the solution via cannula. After 16 h, 10 mL of 1 M NaOH was added, and the aqueous layer extracted with diethyl ether (3x 20 mL). 10 mL 1M HCl was added over ice, and the organic layer extracted with diethyl ether (3x20 mL). The layers were combined and dried with magnesium sulfate and dried to obtain a white solid.

Synthesis of Zr-dCP-Si-2. Zr-dCP-Si-2 dCP was synthesized solvothermally in 9.75mL of DMF. 1 eq (0.276 mmol, 64.3 mg) $ZrCl_4$ was combined with 4 eq (1.104 mmol, 395.2 mg) Si-2, 16 eq (0.736 mmol, 80 μL) water, and 24 eq (6.624 mmol, 324 μL) formic acid. The solution was sonicated for 10 minutes and heated to 80˚C for 120 hours. The resulting dCP powder was washed 3 x 20 mL of DMF and 3 x 20 mL of DCM. The dCP was then dried under vacuum at 120 ˚C.

Exfoliation of Zr-dCP-Si-2. Zr-dCP-Si-2 was exfoliated by sonicating Zr-dCP-Si-2 3D powder in its mother liquor for 6 h. After sonication, it was washed with 3 x 20 mL isopropanol and dried under vacuum.

TCNQ Intercalation into Zr-dCP-Si-2. Tetracyanoquinodimethane (TCNQ) was recrystallized thrice in acetonitrile at 180 ºC for 24 h. TCNQ crystals were collected and dried. Intercalation was accomplished by adding 0.7 eq to 1.0 eq of Zr-Si-2 dCP under vacuum and heated to 200 ºC for 24 h. After 24 h, the dCP changed from a white powder to yellow-green powder.

Figures and Tables

Table S1. Modulator Concentration Effect on Zr-dCP-Si-2 Crystallinity

Modulator	Equivalents	Product
Acetic Acid	0, 6, 12, 24	Gel
Acetic Acid	36	Semi-crystalline powder
Formic Acid	12, 24	Semi-crystalline powder
Formic Acid	36, 72	No product
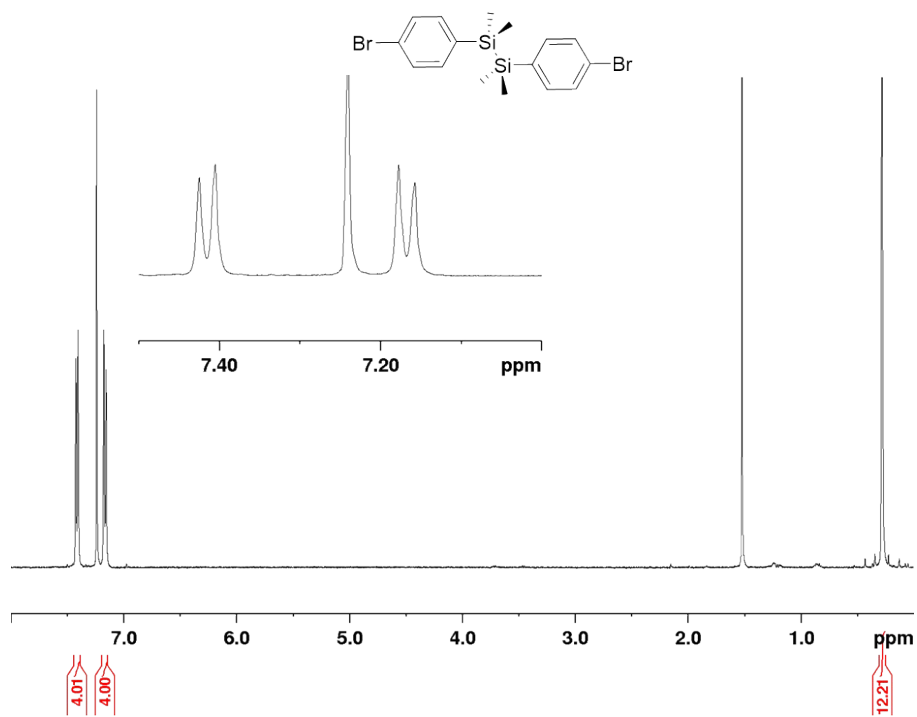
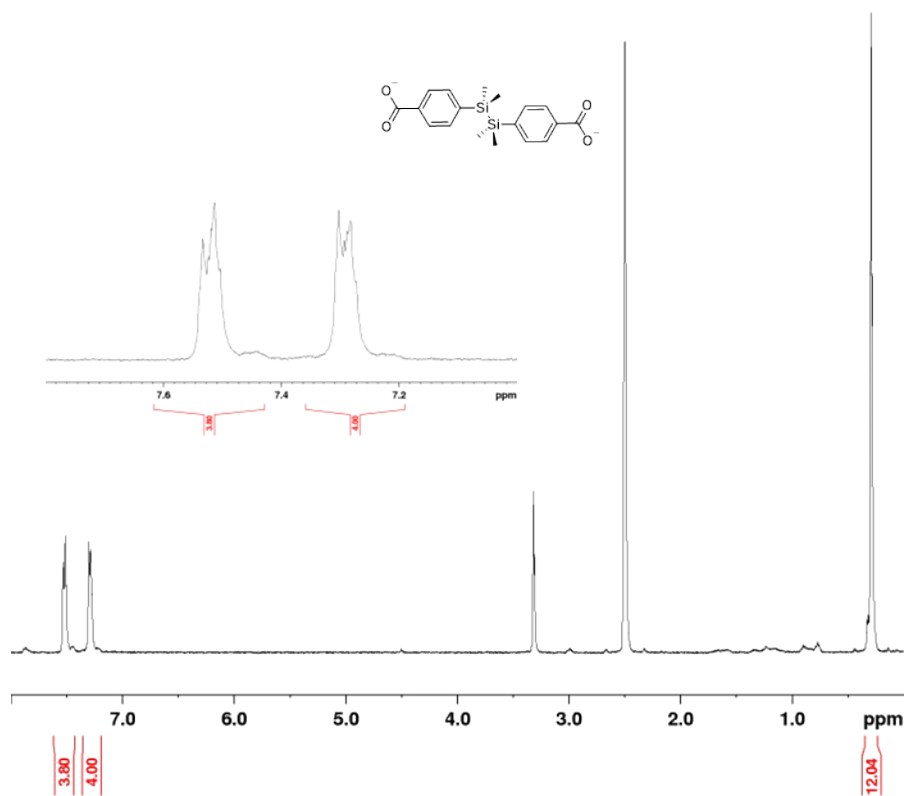**Figure S1.** ¹H NMR of lin-Si-2 precursor (S-2) in CDCl₃.

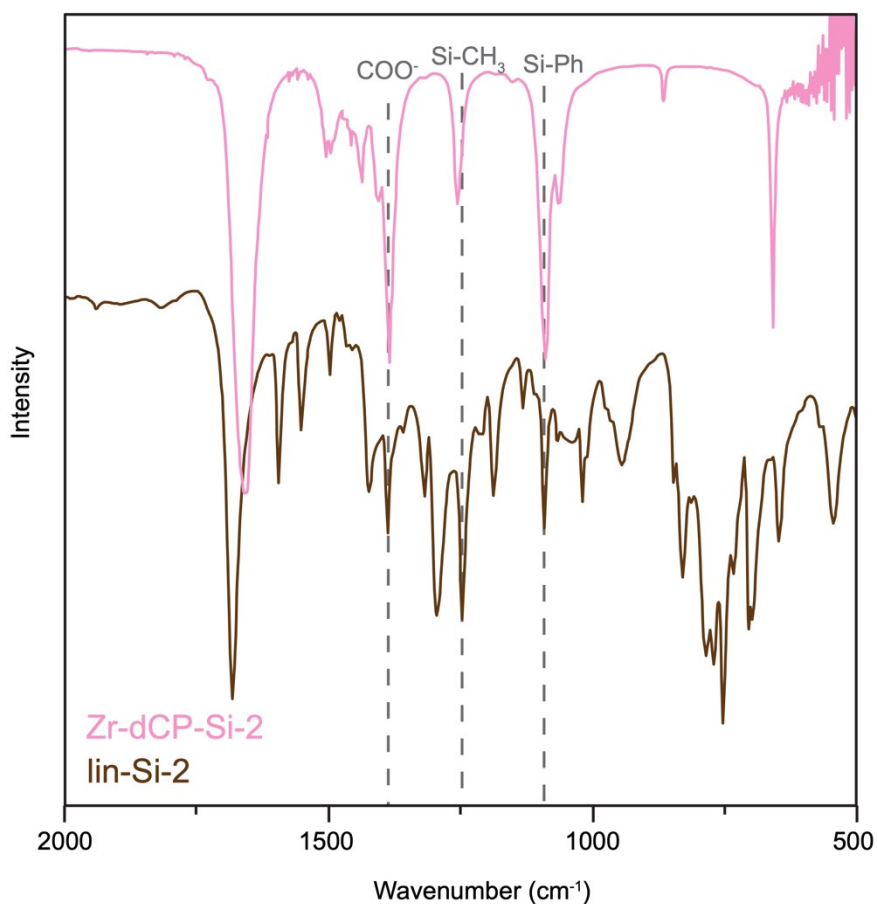**Figure S2.** Full ¹H NMR of lin-Si-2 (S-2) in DMSO.

Figure S3. ATR-IR of lin-Si-2 in comparison with Zr-dCP-Si-2. We note that primary feature indicating metal-ligand bond formation is the red-shift at the C=O interface (~1700 cm^{-1}), associated with the C-O-Zr interface. The blue shift of the Si-CH$_3$ stretch is likely not due to rigidification of the ligand core. Additional gas-phase DFT calculations of the linker in various torsional configurations indicate that linker isomerism is not the origin of the ~5 cm^{-1} blue shift. Instead, we suspect the blue-shift upon forming the metal-linker bond may be due to other interactions not captured in our model. For example, the free linker may be interacting with solvent.
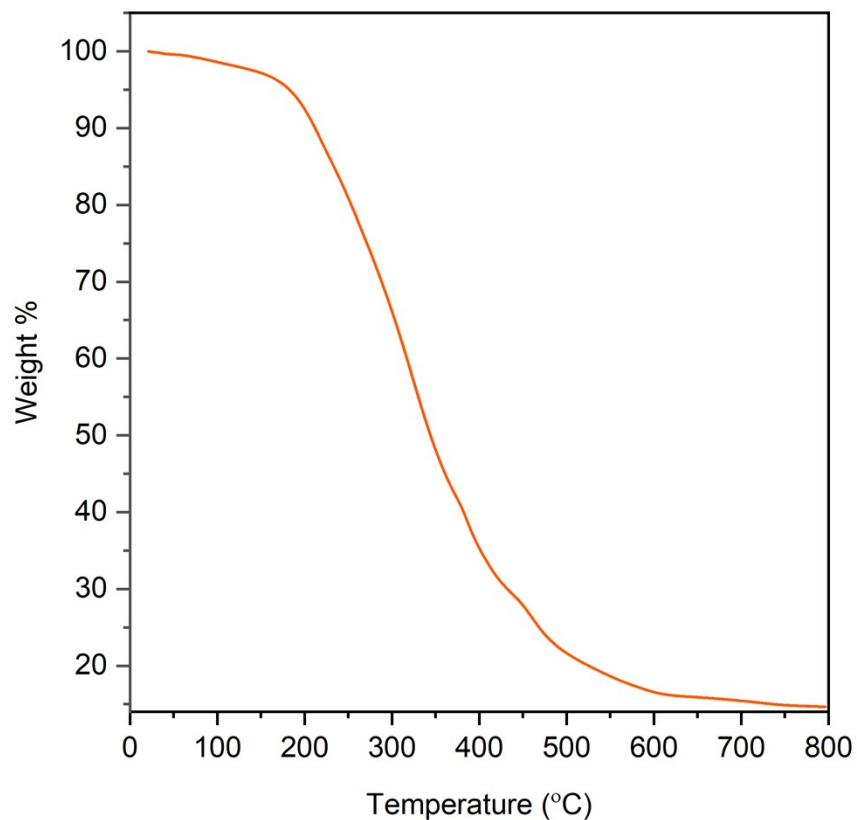
Figure S4. TGA of lin-Si-2. The main loss is at 325 °C and decomposes with 14% of the mass remaining as SiO_2.
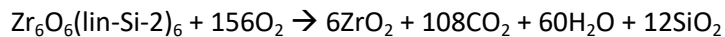
TGA Calculation

Total % of dCP after solvent removed: 83.36%

% of inorganic portion from TGA curve: 48.05%

% of organic portion from TGA curve: 35.31%

Ideal/No defect Zr-dCP-Si-2 Combustion

$Zr_6O_6(lin\text{-}Si\text{-}2)_6 + 156O_2 \rightarrow 6ZrO_2 + 108CO_2 + 60H_2O + 12SiO_2$

Theoretical mass of ideal/no defect Zr-dCP-Si-2: 2779.32 g/mol

Theoretical mass of inorganic portion = $6ZrO_2 + 12SiO_2$ = 1459.2 g/mol

$$173\% = W_{exp} = \frac{Mass\ of\ (Zr_6O_{6-x}(lin-Si-2)_x)}{Mass\ of\ (ZrO_2 + (2x)SiO_2)}$$

$Number\ linkers\ per\ node = \ x = 1.36$

Digestion NMR Calculation

$$\frac{integral\ of\ formate\ from\ NMR}{number\ of\ protons\ in\ formate} \ x \ \frac{number\ of\ aromatic\ protons\ on\ linker}{integral\ of\ aromatic\ protons\ on\ linker\ from\ NMR}$$

$$= \frac{moles\ of\ formate}{moles\ of\ linker} = 2.29$$

The ratio of linker to formate can be calculated based on the digestion NMR to give the number of linkers bound to the node.[2] Assuming we have 6 possible sites per node at which formate or linker molecules can bind, then there are 4.2 formate molecules and 1.8 linker molecules bound per node. When considering the total node coordination (in which two nodes share a linker), there are approximately 8 formate molecules and 4 lin-Si-2 bound to each node.
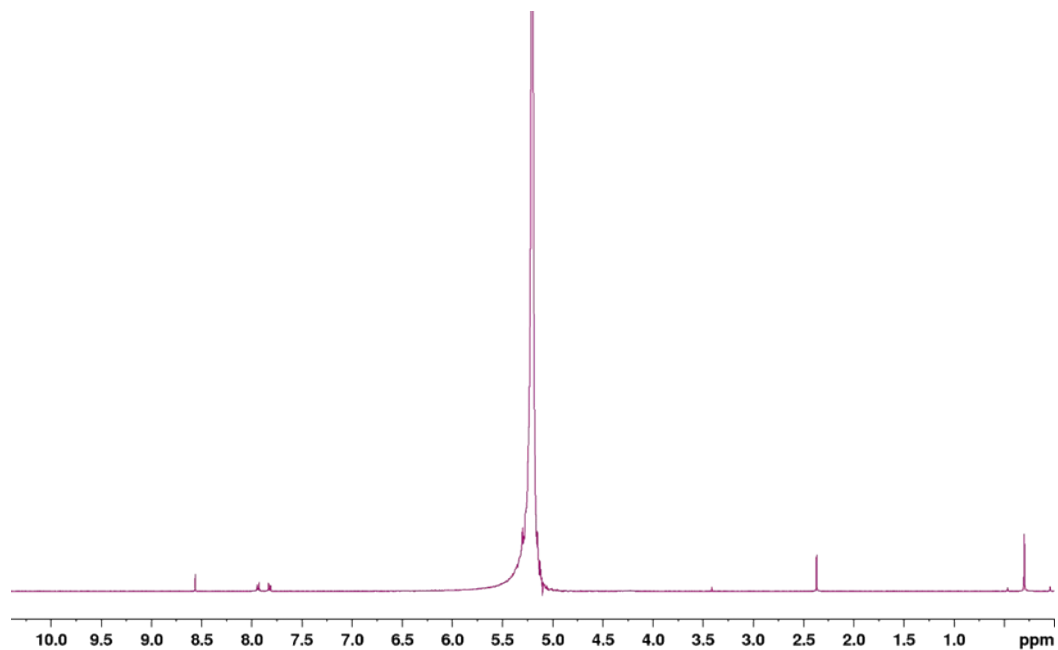

Figure S5. Full ^{1}H NMR of digested Zr-Si-2 dCP. dCP was soaked in concentrated NaOH in D_2O overnight
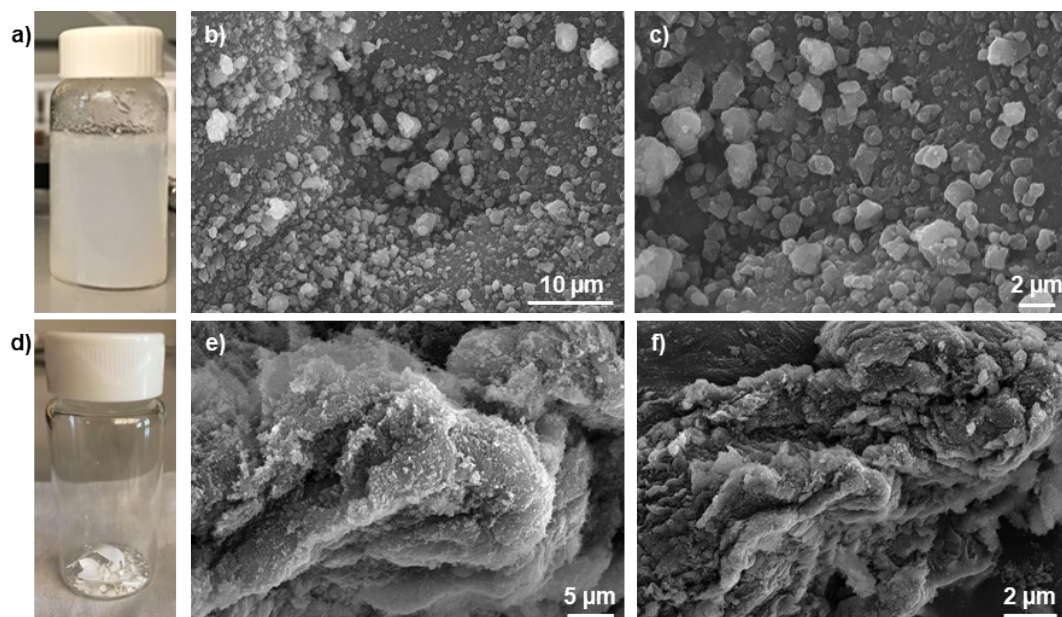
Figure S6. Photographs and SEM images of Zr-dCP-Si-2 **(a-c)** pre- and **(d-f)** post-sonication at different magnifications. The photograph in (a) shows Zr-dCP-Si-2 after solvothermal synthesis (before solvent exchange) as a gel-like material.
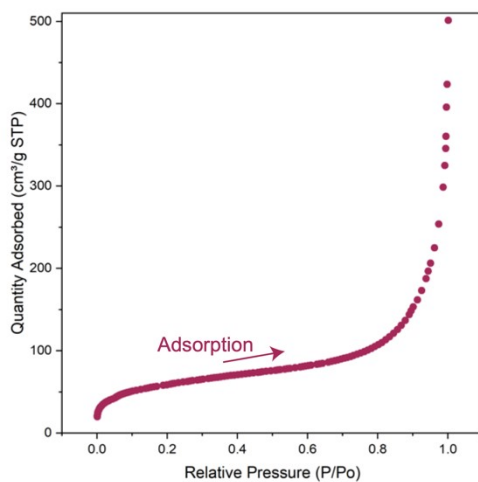

Figure S7: N_2 adsorption isotherm of Zr-dCP-Si-2 at 77 K. The calculated BET surface area was 197.5 m^2 g^{-1}.

Computational Details

Beginning with experimentally determined Zr-clusters common to Zr-based MOFs (UiO-66, NU-1000, **Figure S7c**), a model *b*-oriented 1D-connected coordination polymer was geometrically equilibrated in VASP, using a 500 eV cutoff and a Gamma-centered k-point. The geometry was obtained using the GGA functional, PBEsol. This structure, **Figure 7a,** was then used to simulate PXRD patterns by varying the *a* and *c* lattice parameters.

Electronic structures were obtained by modelling molecular fragments of the extended network. The calculations were performed in Gaussian09. We obtained qualitatively similar energetics using the M06-2X, B3LYP, and HSE06. We elected to include the B3LYP/Def2TZVP data as it has been shown to recover reasonable ionization potentials.[3] The molecular components are shown in **Figure S8**. Electron energies in Figure 7 were aligned with previous literature.[4] Vibrational properties were computed using finite displacements, and corrected using the NIST precomputed scaling factor of 0.965 for B3LYP paired with a triple zeta basis.
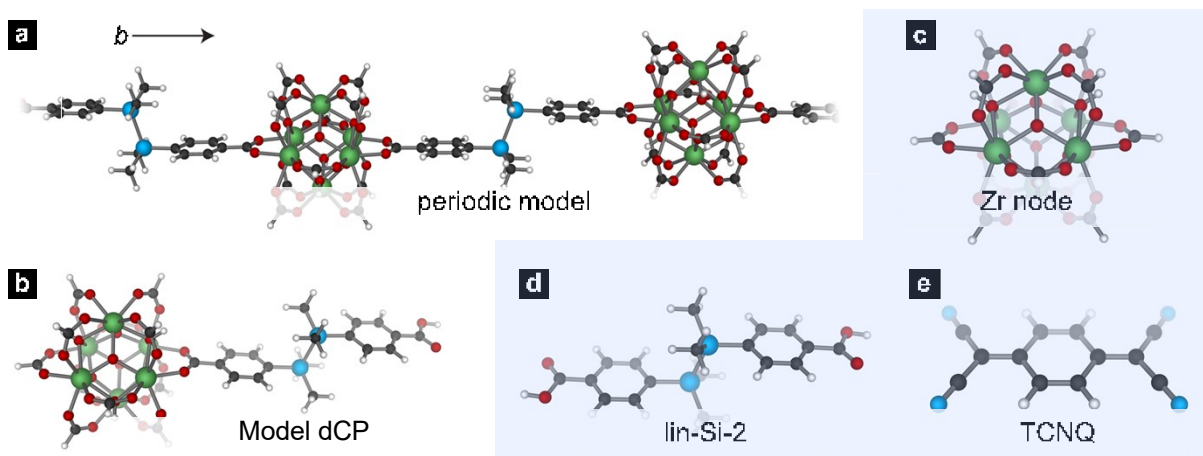

Figure S8. Computational structures. **a**) Periodic 1D chain, containing two Zr clusters and linkers. **b**) Truncated dCP model cluster. **c-e**) Molecular components. The frequency of the C-O stretch in model in **b** was calculated to be 1634 cm^{-1} compared to 1768 cm^{-1} for the free linker.
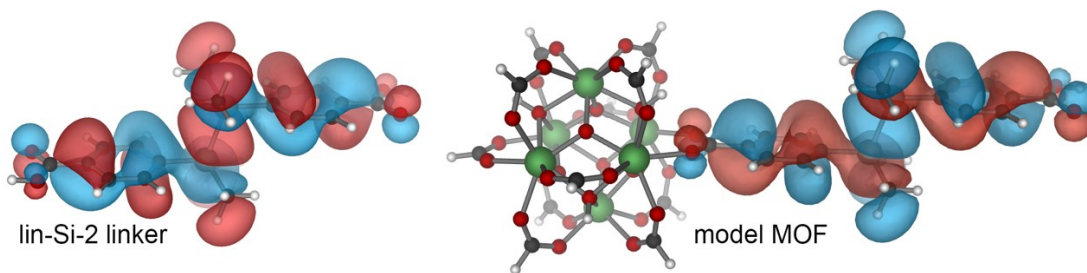
Figure S9. Computed HOMO of lin-Si-2 linker and lin-Si-2 linker bound to a model Zr-formate node. Isosurface is plotted at 0.01 e/Å³.

Table S2. Linear Fits to Tauc Plot for Band Gap Determination

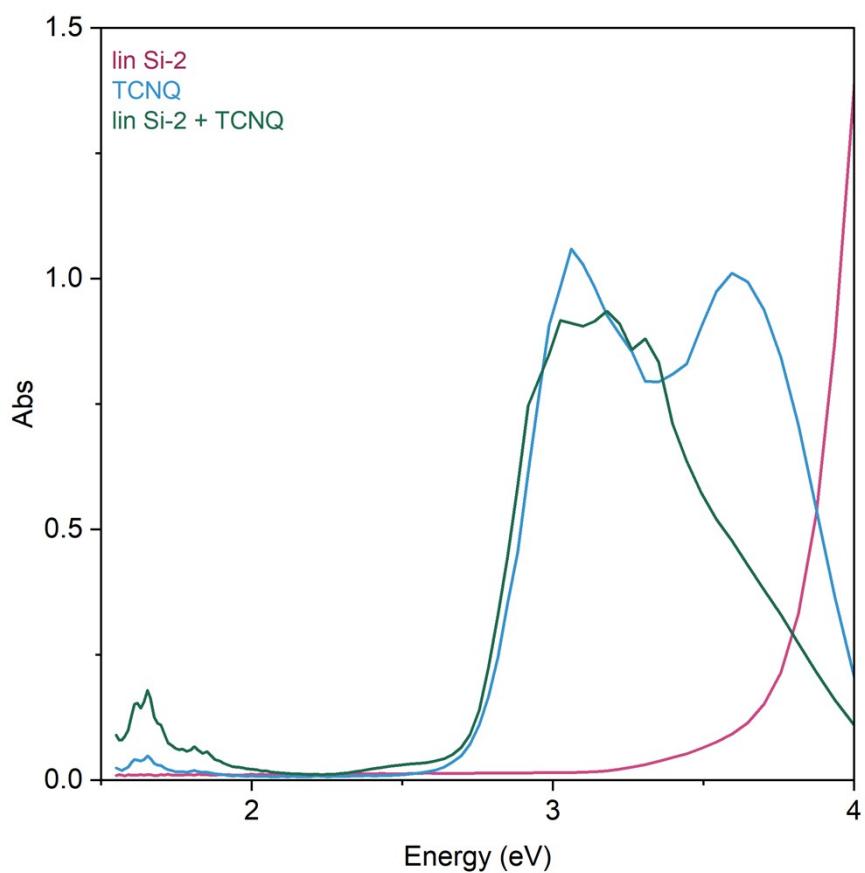| Sample	Linear Fit	Band Gap (eV)
Zr-dCP-Si-2 @ TCNQ	y = 4.58x − 13.5	2.95
TCNQ	y = 5.16x − 15.6	3.02
Zr-dCP-Si-2	y = 111x − 440	3.96
lin-Si-2	y = 27.5x - 112	4.07

Figure S10: Solution-state UV-vis of lin Si-2, TCNQ, and the mixture of linker and TCNQ in solution.
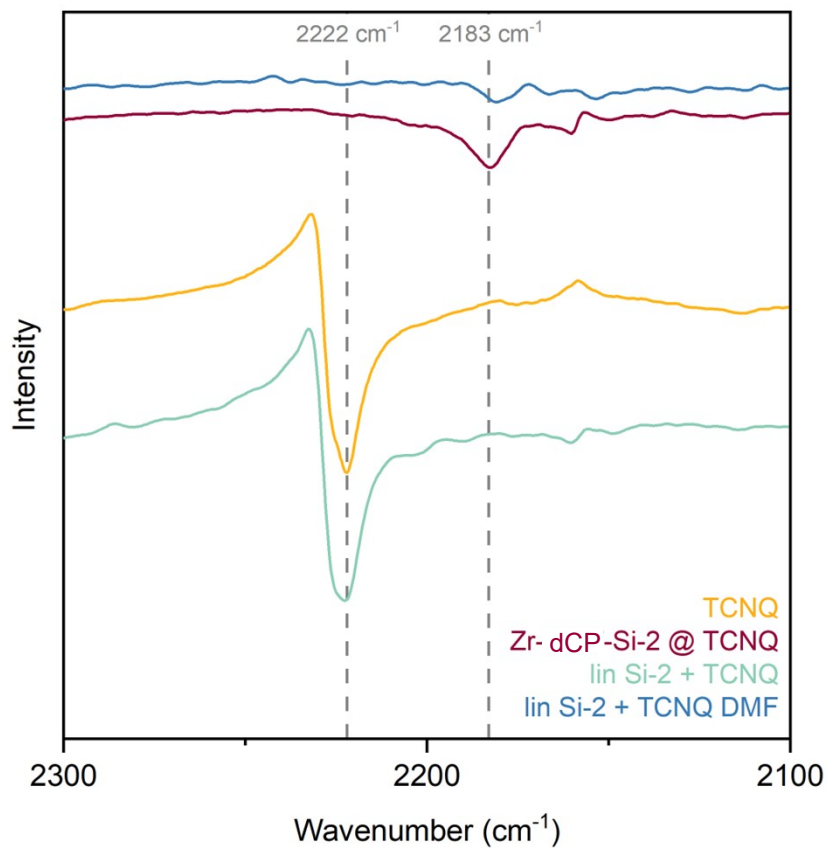
Figure S11: ATR-IR of linker physically mixed (lin Si-2 +TCNQ, green) and mixed in solution (lin Si-2 + TCNQ DMF, blue) in comparison with pure TCNQ (yellow) and the dCP intercalated with TCNQ (red).
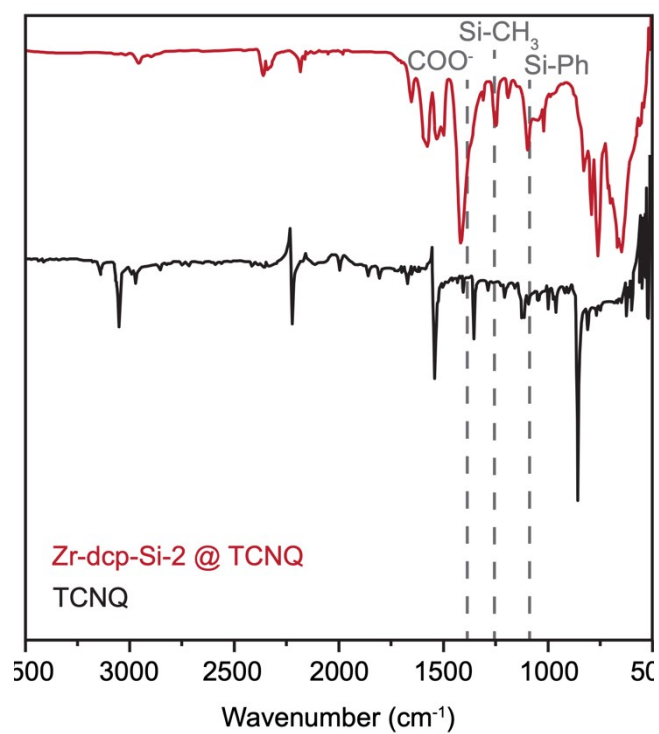
Figure S12. Full ATR-IR of sublimed TCNQ into Zr-Si-2 dCP (dark blue) and TCNQ (light blue).
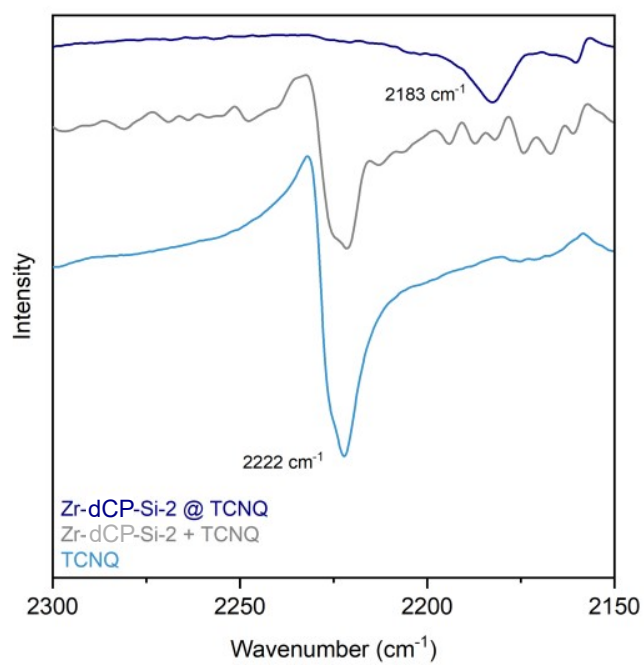

Figure S13. ATR-IR comparison of bare TCNQ (light blue), physically mixed Zr-dCP-Si-2 and TCNQ (gray), and sublimed TCNQ into Zr-dCP-Si-2 (dark blue).
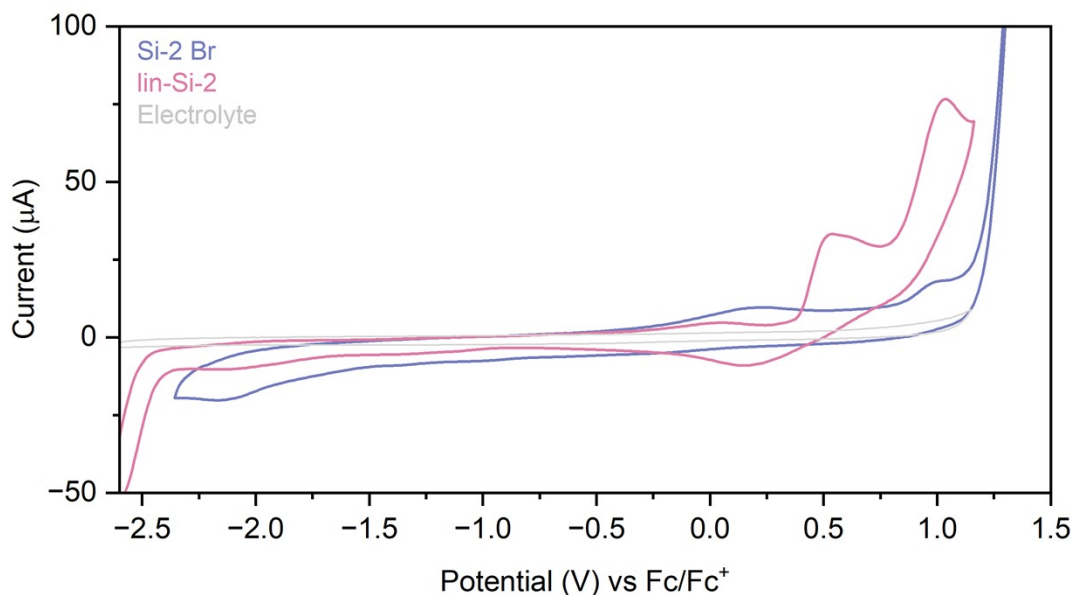
Figure S14. CV of S-2 (brominated precursor to lin-Si-2) in comparison with lin-Si-2. CV was run in a three-electrode cell with a glassy carbon working electrode, Pt wire counter electrode, and Ag wire reference electrode. All CVs were taken with a supporting electrolyte of 0.1 M tetrabutylammonium hexafluorophosphate (TBAPF$_6$) in DMF and cycled at 100 mV s^{-1} and referenced to an external Fc/Fc$^+$ reference. Both CVs exhibit an oxidative peak at 1.04 V vs Fc/Fc$^+$ which agrees with previous literature of analogous compounds.

Table S3 ICP-OES results for Zr and Si content in Zr-dCP-Si-2, reported in mass percent. The result is a ratio of 1 Zr-to-2 Si per mole.

Zr	18.56%
Si	11.38%

References

(1) Burns, A. D. A.; Press, E. M.; Siegler, M. A.; Klausen, S.; Thoi, V. S. 2D Oligosilyl Metal-Organic Frameworks as Multi-State Switchable Materials. https://doi.org/10.1002/anie.201912911.

(2) Shearer, G. S.; Chavan, S.; Bordiga, S.; Svelle, S.; Olsbye, U.; Lillerud, K. P. Defect Engineering: Tuning the Porosity and Composition of the Metal–Organic Framework UiO-66 via Modulated Synthesis Greig. *Chem. Mater.* **2016**, *28* (11), 3749–3761.

(3) Murray, A. T.; Frost, J. M.; Hendon, C. H.; Molloy, C. D.; Carbery, D. R.; Walsh, A. Modular Design of SPIRO-OMeTAD Analogues as Hole Transport Materials in Solar Cells. *Chem. Commun.* **2015**, *51* (43), 8935–8938. https://doi.org/10.1039/C5CC02129D.

(4) Janak, J. F. Proof That $\partial E \, \partial n \, i = \varepsilon$ in Density-Functional Theory. *Phys. Rev. B* **1978**, *18* (12), 7165–7168. https://doi.org/10.1103/PhysRevB.18.7165.

(5) Funabiki, A.; Mochida, T.; Takahashi, K.; Mori, H.; Sakurai, T.; Ohta, H.; Uruichi, M. Reversible Iodine Absorption by Alkali-TCNQ Salts with Associated Changes in Physical Properties. *J. Mater. Chem.* **2012**, *22* (17), 8361. https://doi.org/10.1039/c2jm16821a.

(6) Surampudi, S.; Yeh, M. L.; Siegler, M. A.; Hardigree, J. F. M.; Kasl, T. A.; Katz, H. E.; Klausen, R. S. Increased Carrier Mobility in End-Functionalized Oligosilanes. *Chem. Sci.* **2015**, *6* (3), 1905–1909. https://doi.org/10.1039/c4sc03274h.